

Electric-field-induced orthorhombic phase in $\text{Pb}[(\text{Zn}_{1/3}\text{Nb}_{2/3})_{0.955}\text{Ti}_{0.045}]\text{O}_3$ single crystals

Alexandra-Evelyne Renault,^{a)} Hichem Dammak, Gilbert Calvarin, and Philippe Gaucher
Laboratoire Structures, Propriétés et Modélisation des Solides Unité Mixte de Recherche (UMR)
 8580 Centre National de la Recherche Scientifique (CNRS), Ecole Centrale de Paris, 92295
 Châtenay-Malabry, France

Mai Pham Thi

Thales Research and Technology, Ceramics and Packaging Department, Domaine de Corbeville, 91404
 Orsay, France

(Received 24 August 2004; accepted 21 November 2004)

The ferroelectric phase transitions of $[\bar{1}01]$ -, $[001]$ -, and $[111]$ -oriented $\text{Pb}[(\text{Zn}_{1/3}\text{Nb}_{2/3})\text{O}_3-4.5\%\text{PbTiO}_3$ (PZN-4.5%PT) single crystals were investigated as a function of temperature (T between 300 and 450 K), and electric field (E field between 0 and 300 kV/m) by dielectric and x-ray diffraction combined measurements. Under null E field, PZN-4.5%PT exhibits the following phase transitions: cubic (C) \rightarrow tetragonal (T) \rightarrow rhombohedral (R), during cooling. Under E field applied on a $[\bar{1}01]$ -oriented single crystal, an intermediate orthorhombic (O) ferroelectric phase is induced at temperatures intermediate between that of the T and R phases. The temperature range of existence of this O phase depends both on the crystal orientation and on the measurement conditions: field cooling (FC), zero-field heating after field cooling (ZFHAFC), or field heating (FH). When E field is applied along $[\bar{1}01]$, the stability range is within 40 K in FC and only 15 K in ZFHAFC; when E field is applied along $[001]$ or $[111]$, this range is still narrower. The O phase is not even observed in FH for $[001]$ orientation and in FC for $[111]$ orientation. These observations show that the application of an E field favors the transition to an O phase, leading to a single-domain structure, when the direction of the field is parallel to the spontaneous polarization $[\bar{1}01]$ direction. © 2005 American Institute of Physics. [DOI: 10.1063/1.1849819]

I. INTRODUCTION

The high electromechanical properties of the complex ferroelectric perovskites $A(B'B'')\text{O}_3$, and especially their solid solutions with lead titanate $A(B'B'')\text{O}_3$ -PT near the “morphotropic” phase boundary (MPB) composition, have been the subject of a lot of researches for many decades for practical applications such as ultrasonic imaging for medical diagnostic (echography), underwater communications, and ranging (SONARS). Originally, the MPB was regarded as a simple vertical boundary in the temperature-composition diagram, which separates a ferroelectric rhombohedral (R) phase from a ferroelectric tetragonal (T) one. However, on many complex perovskites, this boundary is curved and corresponds to a phase transition between a low-temperature R phase and a high-temperature T phase. The $T_{R\rightarrow T}$ temperature is composition dependent. The very close value of the free energies of the two ferroelectric phases near the MPB is thought to be the reason for the high electromechanical response in these crystals.¹

More recently, Noheda *et al.*² reported in $\text{Pb}(\text{Zr}_{1-x}\text{Ti}_x)\text{O}_3$ (PZT) ceramics the existence of a monoclinic (M) phase at room temperature (RT), over a narrow composition range, near the MPB. This monoclinic symmetry allows an easy polarization rotation between the antagonist $[111]_R$ and

$[001]_T$ polar axes,³ and thus is responsible for the enhancement of the electromechanical properties observed in PZT near MPB.²

Rhombohedral $\text{Pb}(\text{Zn}_{1/3}\text{Nb}_{2/3})\text{O}_3-x\%\text{PbTiO}_3$ (PZN- $x\%$ PT) single crystals ($0 \leq x \leq 9$), poled along the $[001]$ direction which is different from the $[111]$ direction of the spontaneous polarization, have an ultrahigh electromechanical coupling factor and piezoelectric coefficient ($k_{33}^{[001]} > 90\%$ and $d_{33}^{[001]} > 2000$ pC/N for $x=9$) in the length expansion mode.⁴ The d_{33} value is from 2.5 to 5 times larger than that of PZT ceramics and the maximum electric-field-induced strain is up to 1.7%.⁴ Such an enhancement of the piezoelectric properties was also reported in BaTiO_3 crystal poled along (001) .⁵

However, we showed recently that PZN-9%PT single crystals have a transition temperature $T_{R\rightarrow T}$ relatively close to RT (around 350 K) and exhibit a wide thermal hysteresis around RT,⁶ which makes this compound unsuitable for certain technological applications. So, compositions less close to the MPB, for which the $R \rightarrow T$ phase transition takes place at a higher temperature,^{7,8} have to be considered.

Nowadays, it is also known that the ferroelectric phase-transition sequence of PZN-PT single crystal and their domain configuration at RT strongly depend on the poling orientation and the poling measurement conditions:^{9,10} field cooling (FC), zero-field heating after field cooling (ZFHAFC), and field heating (FH). With regard to PZN-9%PT,

^{a)}Present address: CEA-Saclay, DEN/DMN/SRMA/LA2M, 91191 Gif-sur-Yvette Cedex, France; electronic mail: alexandra.renault@cea.fr

Cox *et al.*¹¹ reported that this compound exhibits a tetragonal (T) \rightarrow orthorhombic (O) phase transition at 350 K; the O cell being B centered, it is equivalent to a primitive monoclinic one (known as M_C), with $a_M = c_M$. More recently, we have shown that the symmetry of PZN-9%PT, at RT, is actually monoclinic M_C , with $a_M \neq c_M$, rather than O .⁶ Notice that the x-ray diffraction study of Cox *et al.*¹¹ was carried out on a polycrystalline sample obtained by grinding a single crystal previously poled along [001], while our x-ray experiments were carried out on real single crystals poled along $[\bar{1}01]$ and [001]. On PZN-4.5%PT, Lu *et al.*¹⁰ reported the following phase-transition sequence: $R \rightarrow T \rightarrow C$ (cubic), from both optical observations and dielectric measurements, using crystals poled along $[\bar{1}01]$, [001], and [111]. On the other hand, from both polarization and strain hysteresis measurements, carried out on the same composition, Ozgul *et al.*¹² and Liu and Lynch¹³ reported that the R phase reversibly transforms into an O phase when submitted to a strong E field applied along $[\bar{1}01]$ at RT.

In order to clarify the phase stability and the phase-transition sequence of PZN-4.5%PT, we carried out dielectric and x-ray combined measurements on single crystals submitted to E fields along $[\bar{1}01]$, [001], and [111].

II. EXPERIMENTAL PROCEDURE

PZN-4.5%PT single crystals were grown by a standard PbO flux method.¹⁴ Three crystals were cut and oriented along the pseudocubic $[\bar{1}01]$, [001], and [111] directions. The sample dimensions were $1.56 \times 1.18 \times 3.58$, $2.86 \times 2.12 \times 0.95$, and $2.09 \times 0.84 \times 1.04$ mm³, respectively. Thin films of Cr/Au electrodes (~ 1300 Å) were, respectively, sputtered on the $(\bar{1}01)$ -, (001)-, and (111)-polished faces.

The dielectric data were recorded at 10 kHz, in FC and ZFHAFC runs, using a HP 4194 impedance analyzer. The displacement current $I(T)$ was measured with a programmable electrometer (Keithley 617) in FH run, in the same experimental conditions, as reported in Ref. 9.

The x-ray diffraction patterns were recorded with a homemade high-resolution two-axes diffractometer,¹⁵ using Cu $K\beta$ ($\lambda = 1.39223$ Å) monochromatic radiation issued from a Rigaku rotating anode (RU300, 18 kW). Samples (single crystal or powder) were fixed on a copper holder inside a N₂ flow cryostat (80–450 K) mounted on a HUBER goniometric head. In the Bragg-Brentano geometry, the diffraction angles were measured with a relative precision better than 0.002° (2θ). Two-dimensional maps of the diffracted intensity were also recorded, rotating the crystal step by step around the ω axis. Such 2θ - ω mappings allow us to characterize the domain structure of the crystals and then to determine its symmetry.⁶

III. RESULTS

A. Phase transitions of a PZN-4.5%PT powder at zero E field

X-ray powder-diffraction patterns were recorded, in cooling run, from 440 to 300 K. The powder sample was

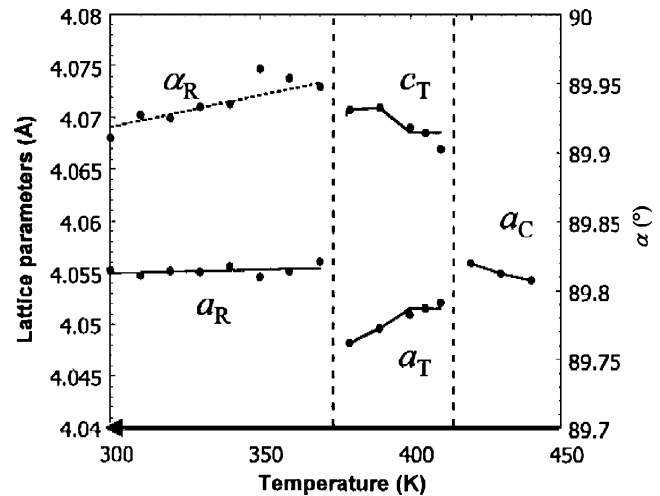


FIG. 1. Temperature dependence of the lattice parameters of PZN-4.5%PT under zero E field, showing the phase-transition sequence: $C \rightarrow T \rightarrow R$, in cooling run.

obtained by grinding single crystals. The powder was sieved ($d \leq 50$ μm) and then annealed at 723 K in order to reduce strains induced by grinding.

Two symmetry changes were revealed by the x-ray patterns: at $T \approx 414(5)$ and $T \approx 374(5)$ K. They correspond to the phase transitions $C \rightarrow T$ and $T \rightarrow R$, respectively. Between these phase-transition temperatures, the lattice parameters change continuously. Figure 1 shows the temperature dependence of cell parameters of C , T , and R phases.

B. Phase transitions of a $[\bar{1}01]$ -poled single crystal

Dielectric measurements were carried out on a $[\bar{1}01]$ -oriented single crystal, in FC ($E = 100$ kV/m). Figure 2 shows the temperature dependence of the permittivity ($\epsilon_{33}^T/\epsilon_0$), at 10 kHz. X-ray investigations were carried out on the same single crystal. Figure 3 shows the temperature dependence of the interplanar spacing d_{303}^- , in FC ($E = 100$ kV/m).

The temperature dependence of $\epsilon_{33}^T/\epsilon_0$ and d_{303}^- both show three abrupt variations, characteristic of phase transitions, at quite comparable temperatures: $T \approx 425(5)$, $385(5)$, $345(5)$ K and $T \approx 432(5)$, $392(5)$, $352(5)$ K, respectively.

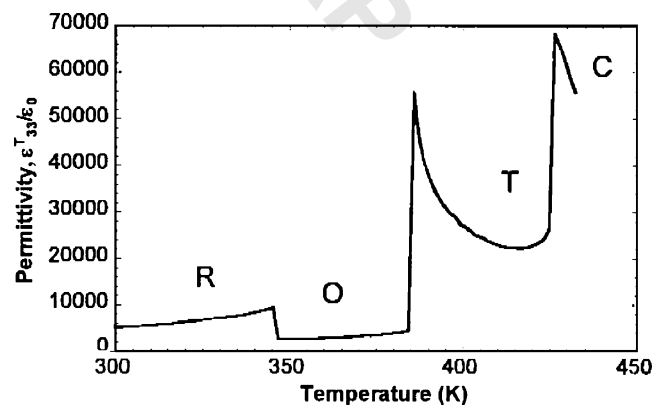


FIG. 2. Temperature dependence of permittivity $\epsilon_{33}^T/\epsilon_0$, measured at 10 kHz in FC ($E = 100$ kV/m), for the $[\bar{1}01]$ -oriented single crystal.

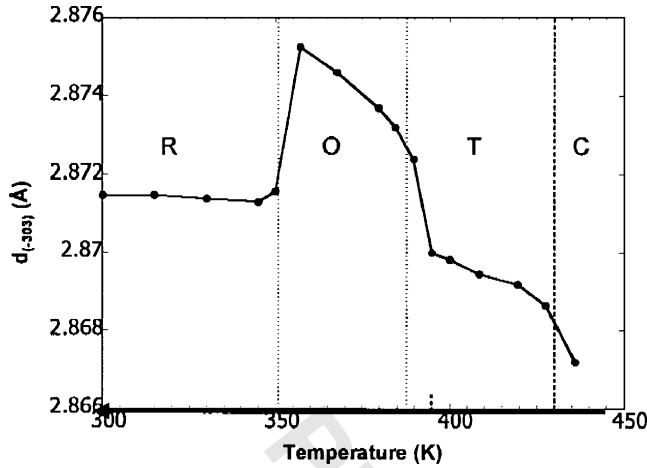


FIG. 3. Temperature dependence of the interplanar spacing $d_{(303)}^*$, measured in FC ($E=100$ kV/m) for the $[\bar{1}01]$ -oriented single crystal.

These results show that an intermediate phase is E field induced between the T and R ones. In the temperature range of this phase, the permittivity $\varepsilon_{33}^{T[\bar{1}01]}/\varepsilon_0$ is lower (Fig. 2) and the interplanar spacing d_{303}^* is higher (Fig. 3) than for the T and R phases. This behavior indicates that the polar axis of the intermediate phase is $[\bar{1}01]$ or close to this direction; in the first case, the phase symmetry is O , and in the second one it is M .

In order to determine the symmetry, O or M , of the intermediate phase, 2θ - ω mappings were recorded, at 383 K, on the three faces $(\bar{1}01)$, (001) , and (010) of the crystal, around the $(\bar{3}03)$, (005) , and (040) reflections, respectively. A single diffraction peak was observed, which means that the intermediate phase is single domain and, consequently, its symmetry is O . Let us remember that for PZN-9%PT, similar mappings revealed the existence of two kinds of domain characteristics of the monoclinic (M_C) symmetry.⁶

The O cell parameters were determined from a least-square refinement of experimental d_{hkl} of $(\bar{3}03)$, (500) , $(\bar{3}33)$, $(\bar{3}13)$, $(\bar{4}02)$, and (040) reflections. The values at 383 K are $a_0=5.737$, $b_0=4.045$, and $c_0=5.746$ Å.

C. Phase transitions as a function of E field applying conditions

It is well known that the phase-transition sequence of PZN-PT crystals strongly depends both on the direction and on the measurement conditions of applied E field.^{9,16} Dielectric constant and displacement current measurements were carried out on $[\bar{1}01]$ -, $[001]$ -, and $[111]$ -oriented crystals following three conditions: FC, ZFHAFC, and FH.

When E field is applied along an off-polar direction, it leads to the setting up of a multidomain configuration which depends on the E field direction. The possible domain configurations of R , T , and O phases which can be E field induced, are schematically represented on Fig. 4. For the E field directions $[001]$, $[\bar{1}01]$, and $[111]$, they were noted: $4O$, $1O$, and $3O$ (O phase); $4R$, $2R$, and $1R$ (R phase); and $1T$, $2T$, and $3T$ (T phase), respectively; the digit stands for the number of equivalent ferroelectric domains.

Temperature dependence of the permittivity ($\varepsilon_{33}^T/\varepsilon_0$) in FC and ZFHAFC is plotted in Fig. 5. The domain configurations of the different phases, for each E field applying direction, were deduced by comparing the values of the dielectric constant. A single-domain configuration exhibits a very low ε_{33} , along the direction of its spontaneous polarization, compared to high ε_{11} and ε_{22} , which are measured perpendicularly to this direction.^{17,18} The effective dielectric constant ε_{33}^* of a multidomain state is a combination of intrinsic dielectric constants ε_i of single domains; consequently, it is much higher than ε_{33} .¹⁸

Figure 5 shows that during FC the intermediate O phase is observed for $[001]$ and $[\bar{1}01]$, and not observed for $[111]$ -oriented crystal. On the other hand, it is important to note that during ZFHAFC the O phase is observed in a temperature range of about 15 K for $[\bar{1}01]$ -oriented crystals.

Figure 6 shows the temperature dependence of the displacement current I during FH on $[\bar{1}01]$ -, $[001]$ -, and $[111]$ -oriented crystals. At 300 K, the domain configuration of a virgin (unpoled) PZN-4.5%PT crystal is $8R$; so, the first current peak observed on the three $I(T)$ curves corresponds to a polarization of this phase: $8R \rightarrow 2R$, $8R \rightarrow 4R$, and $8R \rightarrow 1R$, respectively. The following peaks, at higher temperatures, are due to phase transitions. When the displacement current is positive, the increase in remnant polarization is associated with the structural transition: $2R \rightarrow 1O$ and $4R \rightarrow 1T$, for $[\bar{1}01]$ and $[001]$, respectively. On the other hand, when the displacement current is negative, the polarization of the crystal decreases because of the transition: $1O \rightarrow 2T$ for $[\bar{1}01]$, $1R \rightarrow 3O$ and $3O \rightarrow 3T$ for $[111]$. The last negative current peak corresponds to the total depolarization of the crystal associated with the ferro (T)-paraelectric (C) phase transition.

With $[\bar{1}01]$ -oriented crystals, the phase-transition sequence is similar: $2R \leftrightarrow 1O \leftrightarrow 2T$, whatever the measurement conditions are. The E field-induced O phase is single domain; however, its temperature range of existence depends on the measurement conditions, 40 K under ZFHAFC and 15 K under FC.

With $[001]$ and $[111]$ crystals, the field is in an off-polar direction for the O phase. This phase is induced in a multidomain configuration and its temperature range is so narrow (<10 K) that it is not experimentally observed in FH for $[001]$ and in FC for $[111]$.

D. Phase transitions as a function of E field strength

Dielectric measurements were carried out under FC, with different values of E field, in order to determine the dependence of the stability of the O phase with E field. The transition temperatures, determined from dielectric anomalies, are reported in the E - T diagram (Fig. 7). For $E=0$, the values are those determined by x-ray powder diffraction (Fig. 1). The threshold value to induce the O phase is between 25 and 50 kV/m for $[\bar{1}01]$ and less than 100 kV/m for $[001]$. For $[111]$, the intermediate O phase is not induced, even for $E=300$ kV/m.

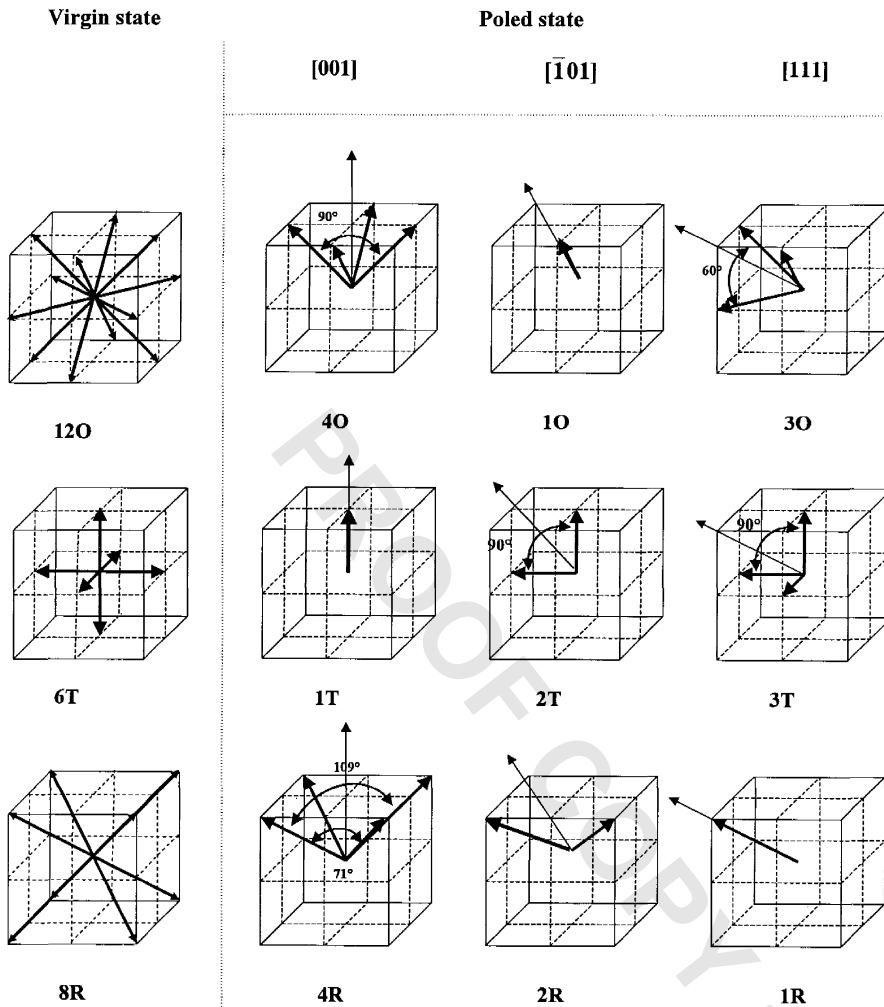


FIG. 4. Schematic representation of the domain configuration of the orthorhombic (*O*), tetragonal (*T*), and rhombohedral (*R*) phases in the virgin and poled states along the $[\bar{1}01]$, [001], and [111] directions (the wide arrows correspond to the direction of the dipolar moments and the narrow ones to the direction of the applied *E* field).

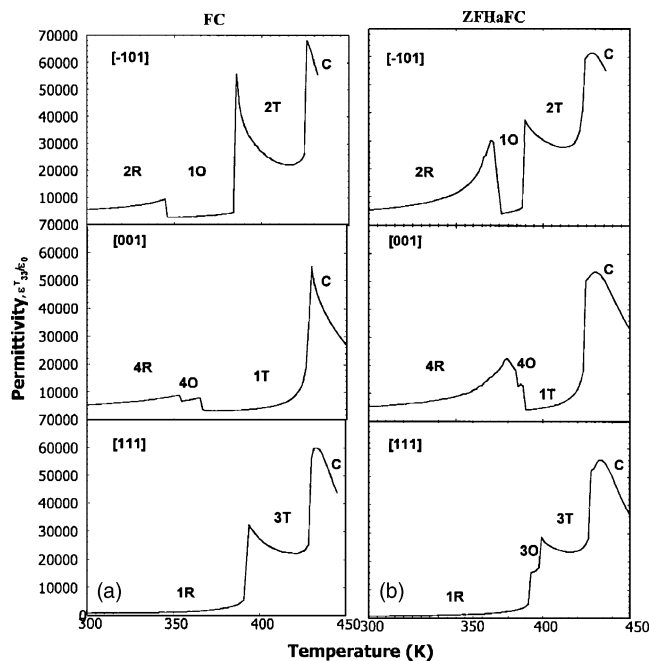


FIG. 5. Temperature dependence of permittivity $\epsilon_{33}^T/\epsilon_0$, measured at 10 kHz in FC ($E=100$ kV/m), and ZFHaFC for the $[\bar{1}01]$ -, [001]-, and [111]-oriented single crystals.

Figure 7 shows as expected that the temperature range of existence of the single-domain state (1*O*, 1*T*, and 1*R*) increases when the electric field is increased; for the 1*O* state, it goes from 23 to 75 K when field increases from 50 to 300 kV/m. For [001], the temperature range of the 4*O* state remains narrow and quasicomstant.

IV. DISCUSSION AND CONCLUSION

At zero *E* field, in cooling run, PZN-4.5%PT exhibits the following phase-transition sequence: $C \rightarrow T \rightarrow R$. Dielectric and x-ray combined measurements, performed under *E* field ($E=100$ kV/m) on $[\bar{1}01]$ -oriented single crystal, showed that an intermediate ferroelectric *O* phase is induced between the *T* and *R* ones.

The temperature range of the induced *O* phase strongly depends both on the direction ($[\bar{1}01]$, [001], or [111]) and on the measurement conditions (FC, ZFHaFC, or FH) of the applied *E* field. When *E* field (100 kV/m) is applied along $[\bar{1}01]$, the polar direction of the *O* phase, its temperature range depends on the measurement conditions: 40 K for FC and 15 K for ZFHaFC. On the other hand, when *E* field is applied along [001] or [111], the temperature range of the *O* phase is much narrower, to such an extent that it is not observed, in our experimental conditions, in FH for [001] and in FC for [111]. For these directions, the *O* phase is expected

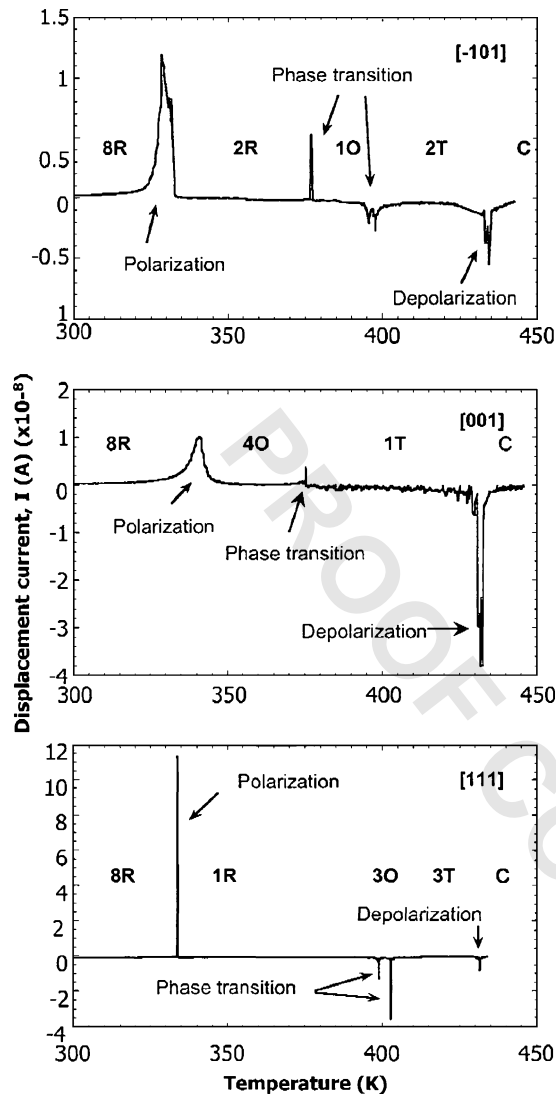


FIG. 6. Temperature dependence of the displacement current $I(T)$, measured in FH ($E=100$ kV/m), for the $[\bar{1}01]$ -, $[001]$ -, and $[111]$ -oriented single crystals.

to be induced in a multidomain configuration, $4O$ for $[001]$ and $3O$ for $[111]$; moreover, in both cases, this multidomain configuration is in competition with a single-domain phase, $1T$ for $[001]$ and $1R$ for $[111]$. So, when the crystal is under E field, the single-domain configuration is energetically promoted because its polarization vector \mathbf{P} is parallel to the field vector \mathbf{E} .

When E field is applied along $[\bar{1}01]$, the temperature range of the O phase increases with E . Assuming a linear dependence of this phase boundary temperature as a function of strength, the O phase should be induced at RT with $E \geq 850$ kV/m. This conclusion agrees with the polarization hysteresis measurements of Liu and Lynch¹³ that showed that the O phase can be E field induced, at RT, with strength over 1000 kV/m.

In conclusion, our results show that an intermediate ferroelectric phase between the T and R phases can be induced by a E field in PZN-4.5%PT; at RT, the stable phase is R . On the other hand, such a behavior has never been observed for PZN-9%PT, the T phase transforms reversibly

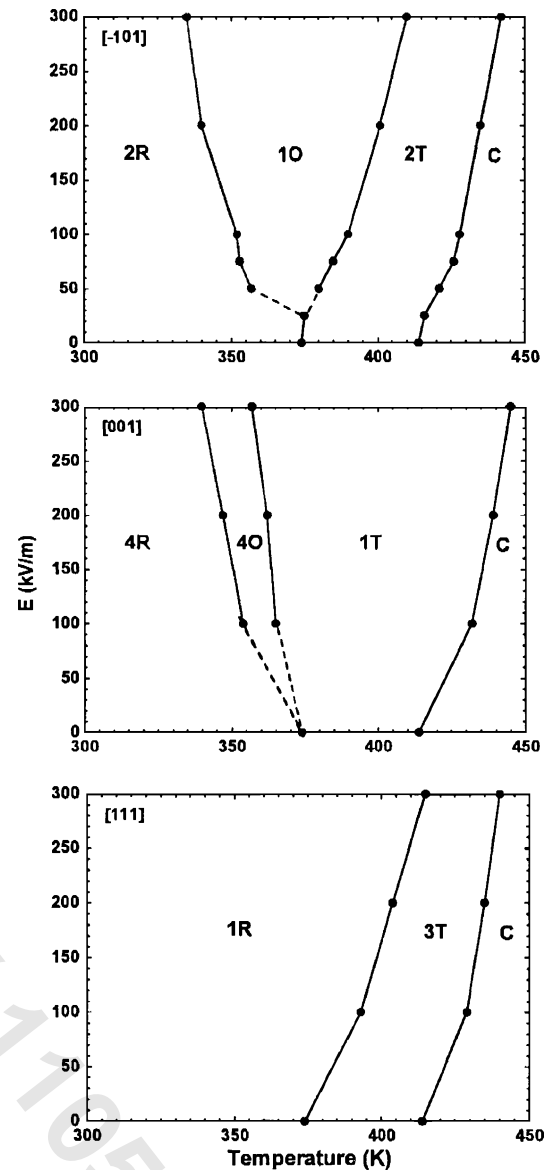


FIG. 7. Field-temperature (E - T) diagrams, resulting from the FC experiments, for the $[\bar{1}01]$ -, $[001]$ -, and $[111]$ -oriented single crystals.

into the monoclinic M_C when the temperature is decreased. Studies are in progress to determine how the phase-transition sequence changes between these two compositions.

- ¹L. Bellaiche, A. Garcia, and D. Vanderbilt, Phys. Rev. Lett. **84**, 5427 (2000).
- ²B. Noheda, J. A. Gonzalo, L. E. Cross, R. Guo, S. E. Park, D. E. Cox, and G. Shirane, Phys. Rev. B **61**, 8687 (2000).
- ³H. Fu and R. E. Cohen, Nature (London) **403**, 281 (2000).
- ⁴S. E. Park and T. R. Shrout, J. Appl. Phys. **82**, 1804 (1997).
- ⁵S. E. Park, S. Wada, L. E. Cross, and T. R. Shrout, J. Appl. Phys. **86**, 2746 (1999).
- ⁶A. E. Renault, H. Dammak, G. Calvarin, M. Pham Thi, and P. Gaucher, Jpn. J. Appl. Phys., Part 1 **41**, 3846 (2002).
- ⁷S. F. Liu, S. E. Park, L. E. Cross, and T. R. Shrout, J. Appl. Phys. **92**, 461 (2002).
- ⁸J. Kuwata, K. Uchino, and S. Nomura, Ferroelectrics **37**, 579 (1981).
- ⁹A. E. Renault, H. Dammak, P. Gaucher, M. Pham Thi, and G. Calvarin, Proceedings of the 13th IEEE ISAF, Nara, Japan (2002) (unpublished), pp. 439-442.
- ¹⁰Y. Lu, D. Y. Jeong, Z.-Y. Cheng, T. R. Shrout, and Q. M. Zhang, Appl.

- Phys. Lett. **80**, 1918 (2002).
- ¹¹D. E. Cox, B. Noheda, G. Shirane, Y. Uesu, K. Fujishiro, and Y. Yamada, Appl. Phys. Lett. **79**, 400 (2001).
- ¹²M. Ozgul, K. Takemura, S. Trolrier-McKinstry, and C. A. Randall, J. Appl. Phys. **89**, 5100 (2001).
- ¹³T. Liu and C. S. Lynch, Acta Mater. **51**, 407 (2003).
- ¹⁴T. Kobayashi, S. Shimanuki, S. Saitoh, and Y. Yamashita, J. Appl. Phys. **36**, 6035 (1997).
- ¹⁵J. F. Bézar, G. Calvarin, and D. Weigel, J. Appl. Crystallogr. **13**, 201 (1980).
- ¹⁶A. Lebon, H. Dammak, and G. Calvarin, J. Phys.: Condens. Matter **15**, 3069 (2003).
- ¹⁷M. Zgonik, R. Schlessler, I. Biaggio, E. Voit, J. Tscherry, and P. Günter, J. Appl. Phys. **74**, 1287 (1993).
- ¹⁸H. Dammak, A. E. Renault, P. Gaucher, M. Pham Thi, and G. Calvarin, Jpn. J. Appl. Phys., Part 1 **42**, 6477 (2003).

PROOF COPY 110503JAP